J Mater Sci: Mater Electron (2016) 27:9861–9869
DOI 10.1007/s10854-016-5054-8

Photodegradation of organic dye by ZnCrLa-layered double hydroxide as visible-light photocatalysts

Mohammad Dinari[1] · Mohamad Mohsen Momeni[1] · Yousef Ghayeb[1]

Received: 24 April 2016 / Accepted: 22 May 2016 / Published online: 27 May 2016

Abstract In this study, lanthanum containing Zn/Cr-Layered double hydroxide (LDH) was synthesis by co-precipitation method and it was used as photo catalyst in the photo degradation of methylene blue. Physicochemical characterization was carried out by X-ray diffraction, Fourier transform infrared, UV–Vis diffuse reflectance spectroscopy, field emission scanning electron microscopy and transmission electron microscopy techniques. Results showed that the photo catalytic activity of Zn/Cr/La-LDH sample is higher than Zn/Cr-LDH sample. Kinetic research showed that the reaction rate constant Zn/Cr/La-LDH is approximately 1.4 times higher than the apparent reaction rate constant of ZnCr-LDH. The stability of the samples was characterized through cyclic photo catalytic test. Results indicated no observable performance degradation for prepared photo catalyst even after four recycles. This work provides an insight into designing and synthesizing new Zn/Cr/La-LDH hybrid materials with good photo catalytic performance.

1 Introduction

Environmental pollutions with various harmful organic compounds are currently one of the most urgent problems that both scientific community and general public face. Thus, different methods for organic decontamination have been studied extensively over the last few decades. However, in context of expensive energy and on-going serious environmental pollution, the search for suitable materials for the removal of organic pollutants, is an important mission of scientific community [1]. A lot of research is being carried out on the development of advanced oxidation processes for wastewater treatment, which usually operate at mild temperature and pressure. Among them, photocatalysis employing semiconductor catalysts has verified their efficiency in degrading refractory organics into readily biodegradable compounds, and ultimately mineralizing them into innocuous CO_2 and H_2O [2]. But, the greater part of the frequently used photocatalysts like TiO_2 cannot be activated by visible light due to their large band gap, resulting in low photo-electronic conversion efficiency [3–5]. As visible light occupies the largest proportion of the solar spectrum, much attention in photocatalysis has been focused on the photocatalytic degradation of organic pollutants under visible light irradiation, which is one of the most promising ways for environmental issues [6–8]. Therefore, developing new materials with high efficiency has become a hot topic in order to improve the efficiency of degradation of dye and other molecules using just sunlight [9, 10].

Along with the alternate semiconductor photocatalysts that have been investigated to date, layered double hydroxide (LDH)-based photocatalysts have emerged as a very promising candidate to replace TiO_2, owing to their unique layered structure, tunable band gaps, low cost, ease of scale-up, and good photocatalytic activity for water splitting and other reactions [11–16]. As one kind of useful multi-functional layered materials, LDH as have attracted much attention owing to their potential applications in catalysts, medicine, adsorption, ion exchangers, electrical functional materials and organic–inorganic nanocomposites [17–19].

✉ Mohammad Dinari
dinari@cc.iut.ac.ir; mdinary@gmail.com

✉ Mohamad Mohsen Momeni
mm.momeni@cc.iut.ac.ir

[1] Department of Chemistry, Isfahan University of Technology, Isfahan, 84156-83111, Islamic Republic Iran

On account of its relatively high surface area and anion exchange capacities, it has been used to treat toxic metals and anionic dyes [20–23]. The novelty of eco-compatible LDHs lies in their simple synthetic procedures, high level of purity, ability to be organo-modified with a variety of organic ions, versatility in chemical composition and multiple interactions with other compounds [24, 25]. The general chemical composition of LDH can be represented as $\left[M^{2+}_{1-x}M^{3+}_{x}(OH)_2\right]\left[(A^{n-})_{x/n}\cdot mH_2O\right]$, where M^{2+} and M^{3+} represent di- and trivalent metal ions within the brucite-like layers respectively, and A^{n-} is an interlayer anion. According to the formula, it is possible to obtain a great variety of LDH by solely changing the nature and proportions of the metallic cations in the hydroxyl sheets and by the intercalation of various solvated anions in between the layers [26–29].

Numerous investigations on the application of LDHs based photocatalysts by incorporating particular photoactive metal cations into LDHs for the elimination of organic pollutants using artificial UV or solar light as the irradiation source have been reported. Surface defects can be introduced by controlling the particle size, which change the LDH electronic structure and greatly enhance the efficiency of photogenerated charge separation and photocatalytic reactions rates [30–32].

Transition metal oxides have indicated good potential catalytic properties; while the rare earth element La based compounds including Lanthanum oxide and hydroxide have shown better potentials for adsorption of arsenic from aqueous solutions, lubricant additives [33–35]. How to take advantage of the particular characteristics of LDH materials and transition metal oxides including rare earth elements for photocatalytic reactions, it is important for the design and synthesis of novel materials for elimination of organic pollutants.

We have synthesized Zn/Cr-LDH and Zn/Cr/La LDHs by coprecipitation method. Methylene blue (MB) decomposition reactions under visible light irradiation were used in this study to evaluate the photocatalytic activities of the obtained LDH. The structural, morphological, textural and semiconducting properties of as-synthesized solids were confirmed by UV–Vis DRS, field emission scanning electron microscopy (FE-SEM) and transmission electron microscopy (TEM), X-ray diffraction (XRD), Fourier transfer infrared (FTIR), and UV–Vis techniques. The photocatalytic degradation experiments with Zn/Cr/La-LDH composite were conducted to show that a higher visible-light-driven degradation of organic pollutants could be obtained. Zn/Cr/La-LDH composite photocatalyst exhibited much high photo catalytic activity as compared to Zn/Cr-LDH alone.

2 Experimental

2.1 Materials

Zinc nitrate hexahydrate [$Zn(NO_3)_2$.$6H_2O$], Chromium nitrate nonahydrate [$Cr(NO_3)_3$.$9H_2O$], Lanthanum(III) nitrate hexahydrate [$La(NO_3)_3$.$6H_2O$] NaOH and Na_2CO_3 were purchased from Aldrich Chemical Co. All chemicals were commercial materials of the highest available purity and they were used as received.

2.2 Preparation of layered double hydroxide

Co-precipitation method was used for the synthesis of the Zn/Cr/La-LDHs First, a mixture of 1.0 g of $Zn(NO_3)_2\cdot 6H_2O$, 0.27 g of $Cr(NO_3)_3\cdot 9H_2O$ and 0.2 g of $La(NO_3)_3\cdot 6H_2O$ (Zn:Cr:La = 2.0:0.7:0.3 molar ratio) was dissolved in certain volume of deionized water. Then the above solution and a mixture containing NaOH (2 M) and Na_2CO_3 (0.5 M) were added simultaneously to a three-necked flask at a speed of 1 drop s^{-1}. The pH of resulting suspension was maintained at 9–10 by continuous addition of a 1 M NaOH and the mixed solution stirring for 12 h. Finally, the mixture was transferred to Teflon-lined stainless steel autoclaves and the hydrothermal temperature is 160 °C for another 24 h. The resulting solid product was separated by centrifugation, washed with deionized water several times until pH = 7, and dried in an oven at 80 °C for 6 h. This solid was labeled Zn/Cr/La-LDH.

Zn/Cr-LDH with 2.0:1.0 molar ratios was prepared by similar procedure without using $La(NO_3)_3$.$6H_2O$.

2.3 Photo catalytic experiments

Photo catalytic activities of all the samples were evaluated by degradation of the aqueous methylene blue (MB) as model pollutant under visible light irradiation. Methylene blue is a cationic dye, used extensively for dying cotton, wool and silk. The risks of the existence of this dye in waste water have arisen from the burns effect of eye, nausea, vomiting and diarrhea. MB has a maximum absorption in the 660 nm visible area. Methylene blue is chosen as a model contaminant to evaluate the photocatalytic activity of prepared samples due to its stability under visible light irradiation. Chemical structure of methylene blue ($C_{16}H_{18}N_3SCl$) makes it to fall under a group of azin dyes. The photo catalytic reaction was carried in a single-compartment cylindrical quartz reactor. A 200 W xenon lamp was used as a light source. The luminous intensity of the xenon lamp was 100 mW/cm^2. The actual experiments were performed at room temperature. The initial concentration of MB was 2 mg/L and 20 mg as-prepared photo

catalysts were added and then stirred with a magnetic bar. Prior to illumination, the solution containing MB and photo catalyst magnetically stirred for 120 min in the dark to ensure the establishment of an adsorption–desorption equilibrium between the photo catalyst and MB. Then the solution was exposed to light irradiation under magnetic stirring for 120 min. At certain time intervals, specific amount of the solution was withdrawn and the changes in concentration of MB were observed using a UV–Vis spectrophotometer.

2.4 Characterization techniques

XRD (Philips X' Pert Pro-MPD) studies were performed to identify the formation of crystal phase by using Cu $K\alpha$ radiation ($\lambda = 0.1542$ nm). The diffraction patterns were collected between 2θ of 5° and 80° at a scanning rate of 0.05°/min. The scanning speed was 0.02°/s. FT-IR spectra were recorded on Jasco-680 (Japan) spectrophotometer with 4 cm^{-1} resolution. The KBr pellet technique was applied for monitoring changes in the FT-IR spectra of the samples in the range of 4,000–400 cm^{-1}. The vibrational transition frequencies are reported in wave numbers (cm^{-1}). The morphology of the samples was examined by FE-SEM (HITACHI; S-4160) which was connected with an energy dispersive spectroscopy (EDS). The powdered sample was dispersed in H_2O, and then the sediment was dried at room temperature before gold coating. Transmission electron microscopy (TEM) images of the samples were collected on a Philips CM120 transmission electron microscope with accelerator voltage of 100 kV. The UV–Vis absorption spectra were recorded using UV–Vis-NIR spectrophotometer with an integrating sphere (DUV-3700, Shimadzu, Japan), which $BaSO_4$ was used as a reference.

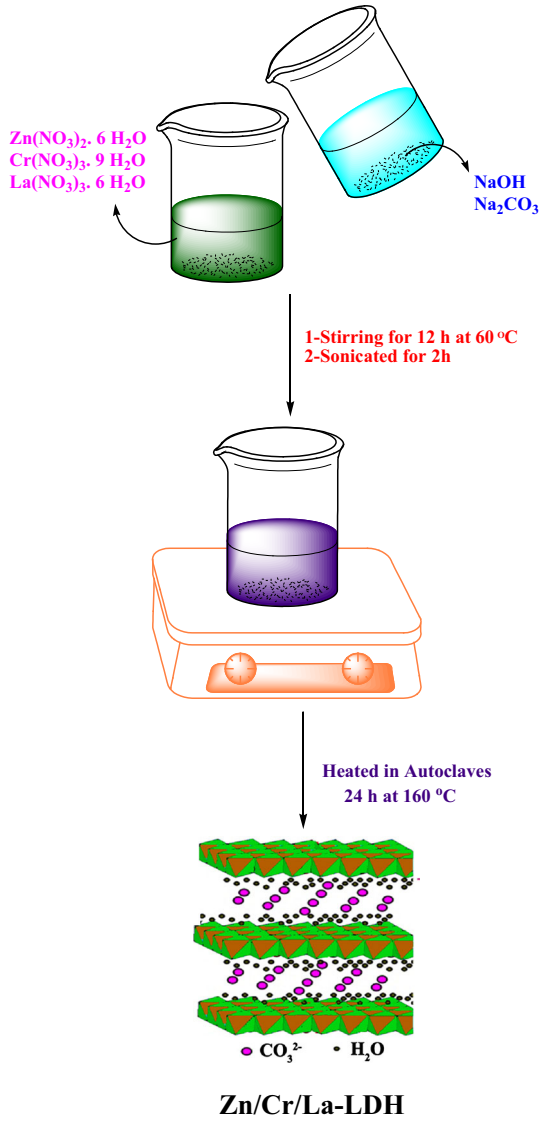

Scheme 1 Synthesis of Zn/Cr/La-LDH

3 Results and discussion

The reaction pathways for the synthesis of Zn/Cr/La-LDH by co-precipitation method are shown in Scheme 1.

3.1 FT-IR study

FT-IR spectra of Zn/Cr-LDH and Zn/Cr/La-LDH are shown in Fig. 1. LDH containing CO_3^{2-} anions have characteristic bands for various modes of infrared sensitive vibrations of the anion [25–27]. In these spectrum, the broad absorption band in the region 3100–3600 cm^{-1} is assigned to the OH stretching vibrations, ν(OH), associated with the basal hydroxyl groups and interlayer water. The bending vibration of the interlayer H_2O is also reflected in the broad bands around 1620 cm^{-1}. The O-C-O asymmetric stretching vibration appears between 1363 and 1507 cm^{-1}. Compared with CO_3^{2-} of $CaCO_3$ (1430 cm^{-1}), there is a considerable lower shifted absorption peak at 1365 cm^{-1}, shows that there was an intercalation between CO_3^{2-} and interlayer H_2O through the strong hydrogen bonding. The bands at lower wavenumbers such as 792 cm^{-1}, 552 cm^{-1} and 431 cm^{-1} can be assigned to the metal–oxygen stretching modes (Zn–O, Cr–O). In the case of Zn/Cr/La-LDH, the bands recorded in the low-frequency region of the spectrum (< 600 cm^{-1}) can be interpreted as lattice vibration modes such as M–O-H vibration and O-M–O stretching. These results confirmed the formation of LDHs (Fig. 1).

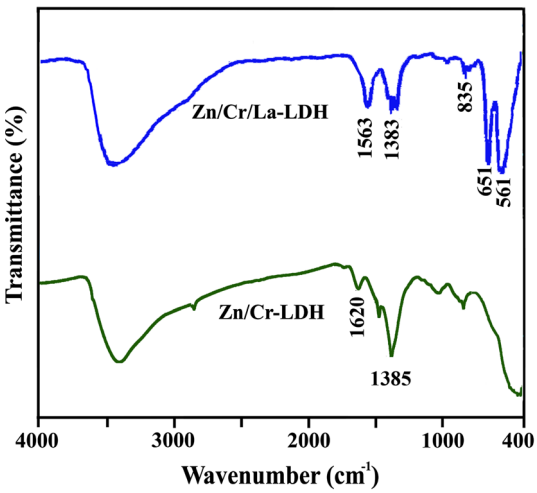

Fig. 1 FT-IR spectra of the Zn/Cr-LDH and Zn/Cr/La-LDH

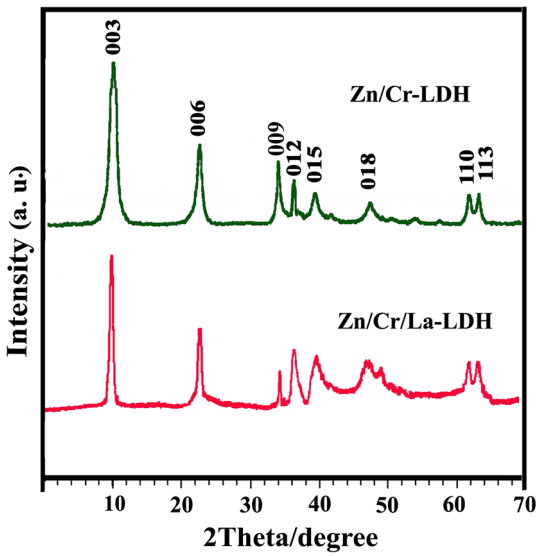

Fig. 2 XRD patterns of the Zn/Cr-LDH and Zn/Cr/La-LDH

3.2 X-ray diffraction

The XRD patterns of the synthesized Zn/Cr-LDH and Zn/Cr/La-LDH samples showed a typical layered double hydroxide structure. In the Zn/Cr-LDH sample, the sharp and symmetric reflections for (0 0 3), (0 0 6), (1 1 0) and (1 1 3) planes and broad asymmetric peaks for (0 0 9), (0 1 5) and (0 1 8) planes, which are characteristic planes of HT-like materials with hexagonal crystal system assuming a 3R packing of layers [36]. The sharpness and intensity of the reflections, as a measure of crystallinity, decreased in the Zn/Cr/La-LDH due to the presence of La^{3+} ions. The high electric charge of La^{3+} favored the formation of related carbonate and oxy-hydroxide lanthanum species at the early stage of the co-precipitation [37]. The possible reason may be related to the different ratios of electric charge to radius for different metal ions. The average crystalline size of Zn/Cr-LDH and Zn/Cr/La-LDH samples, which has been determined from the half width of the diffraction using the Debye–Scherrer equation ($D = K\lambda/\beta cos\theta$) is approximately 34 nm and 26 nm, respectively, where D is the crystallite size, λ is wavelength of the radiation, θ is the Bragg's angle and β is the full width at half maximum [38] Fig. 2.

3.3 FE-SEM and EDX study

The FE-SEM images and EDS patterns of the Zn/Cr-LDH are shown in Fig. 3. In general, LDH crystal has plate-like morphology and hexagonal crystallite. It is found that this sample showed the characteristics of plate-like morphology and hexagonal crystallite of LDH materials. The particle size distribution indicates that the size of LDH nanoparticles mainly ranges from 25 to 50 nm. Moreover, as shown in Fig. 3, the EDS pattern of the Zn/Cr-LDH indicates the elements of Zn and Cr and confirmed the formation of the LDH.

Figure 4 shows the FE-SEM images as well as the EDS pattern of the Zn/Cr/La-LDH. The sample also showed the nature of LDH particles, which roughly consists of plate-like shape as well as spherical shape, stacked with smooth surface in which is formed of irregular aggregates. These figures show that the diameter distribution of LDH particles were narrow and they have the diameter about 30–40 nm. The presence of La in the LDH was also confirmed by EDS techniques as shown in Fig. 4.

3.4 TEM study

TEM picture presented an actual image of nanoclay platelets to permit recognition of internal morphology of nano-hybrids. Figure 5 shows the TEM image of Zn/Cr-LDH and Zn/Cr/La-LDH samples with different magnifications. According to the TEM pictures, both samples have smooth overlapping crystals, and they are approximately in hexagonal form with uniform thickness which was commonly observed for typical LDH compounds. For Zn/Cr/La-LDH, the plate size is smaller than another sample without La (Fig. 5). According to the TEM images, the particles size of the Zn/Cr-LDH and Zn/Cr/La-LDH are 15–25 and 10–18 nm, respectively and these results are in consisted with the XRD patterns of the LDH samples.

3.5 Optical measurements

The light absorbance of the Zn/Cr-LDH and Zn/Cr/La-LDH samples was evaluated by the UV–Vis diffuse reflection absorption spectra and the results are shown in

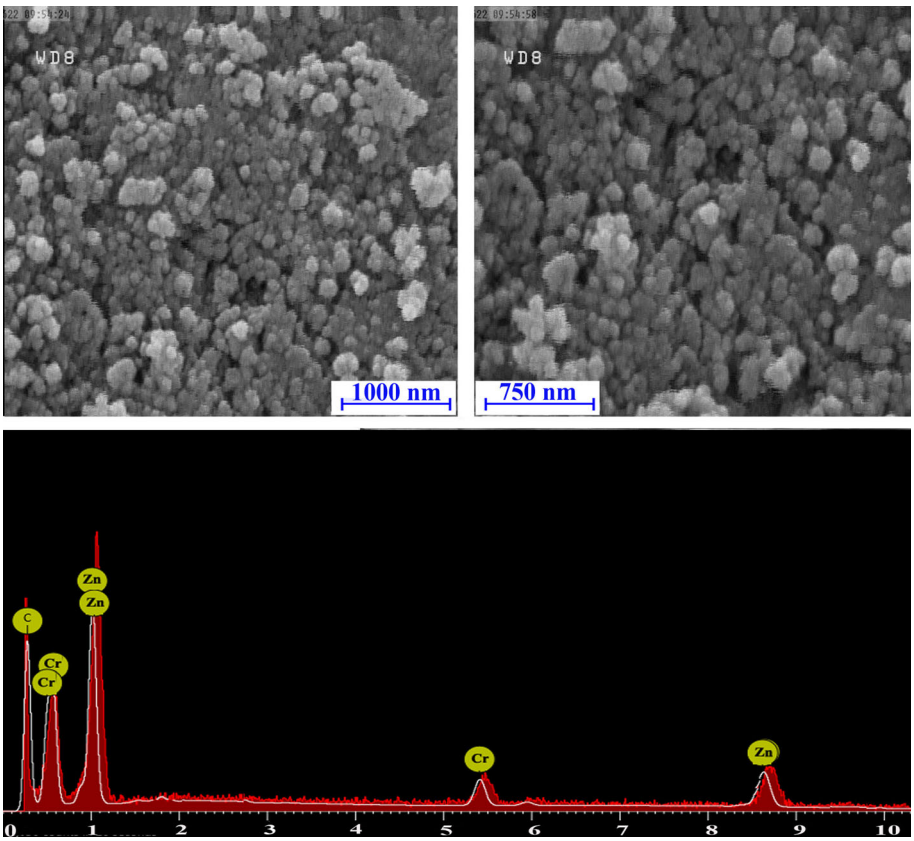

Fig. 3 FE-SEM photographs and EDS pattern of the Zn/Cr-LDH sample

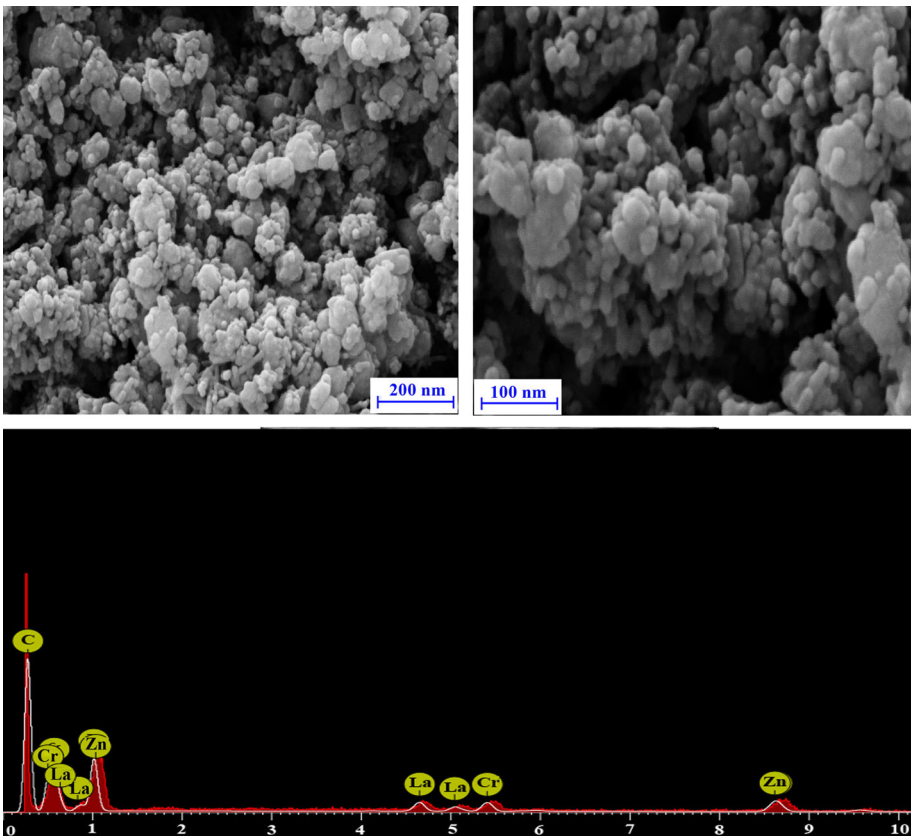

Fig. 4 FE-SEM photographs and EDS pattern of the Zn/Cr/La-LDH sample

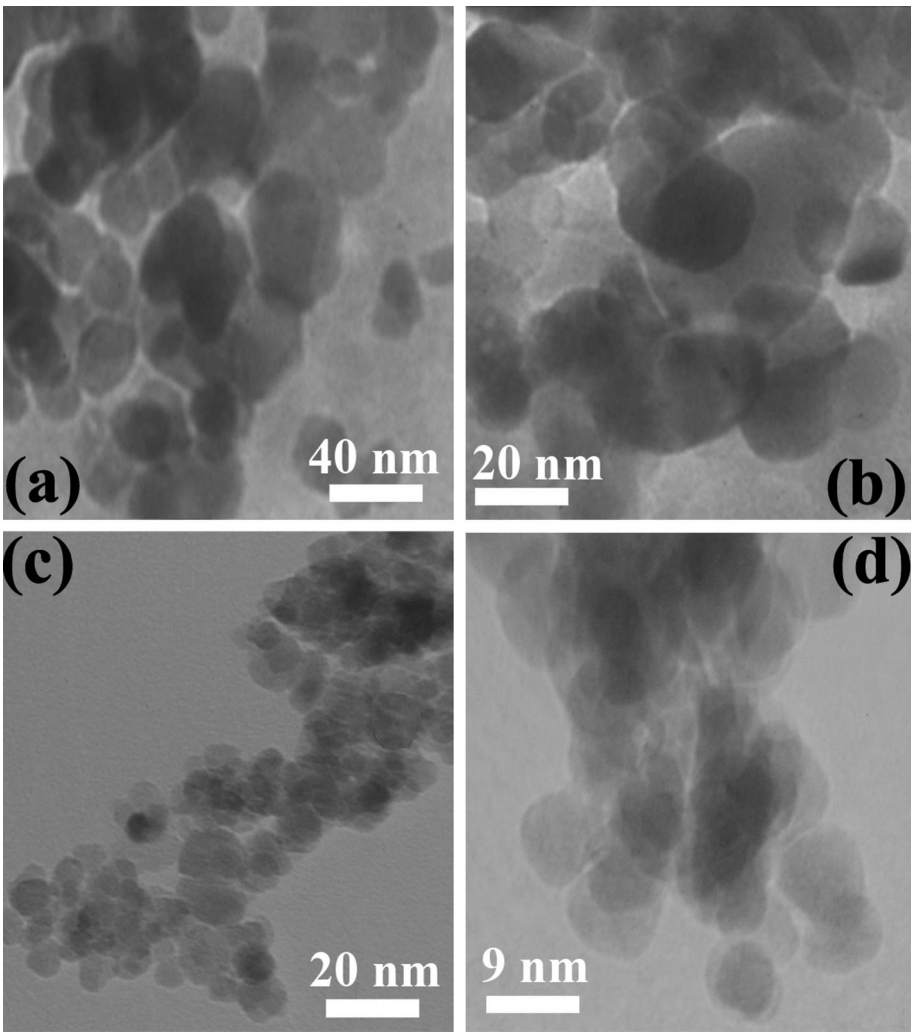

Fig. 5 TEM micrographs of the (**a**, **b**) Zn/Cr-LDH and (**c**, **d**) Zn/Cr/la-LDH

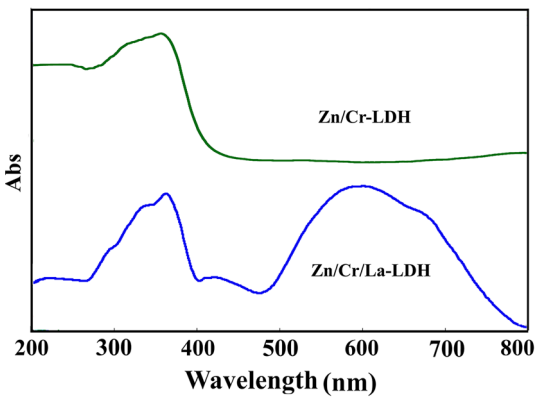

Fig. 6 UV–Vis spectra of the ZnCr-LDH and Zn/Cr/La-LDH

Fig. 6. The strong absorption band in the region of 394 nm for Zn/Cr-LDH, can be assigned to typical in Zn(II) coordinated to the CO_3^{2-} gallery [28–30]. In the case of Zn/Cr/La-LDH, absorption at 586 nm was observed and confirmed the presence of La^{3+} in the brucite like sheets. The broad nature of absorption at ~ 600 nm could be ascribed to supramolecular guest–guest (hydrogen bonding and van der Waals forces) or guest–host interactions (electrostatic attraction, hydrogen bonding and van der Waals forces) [28–30]. In case of the layered materials, the UV spectrum shows an overall broadening and a red shift is observed due to higher aggregate formation.

3.6 Photo catalytic activity of Ni/Cr-LDH and Ni/Cr/La-LDH samples

Photo catalytic activity of different samples was followed through degradation of methylene blue as a function of irradiation time with Xe light. To get the response of photo catalytic activities of Zn/Cr-LDH and Zn/Cr/La-LDH samples, the absorption spectra of exposed samples at various time intervals were recorded and the rate of color degradation was observed in terms of change in intensity at λmax of the dye. The photo degradation yield is defined as:

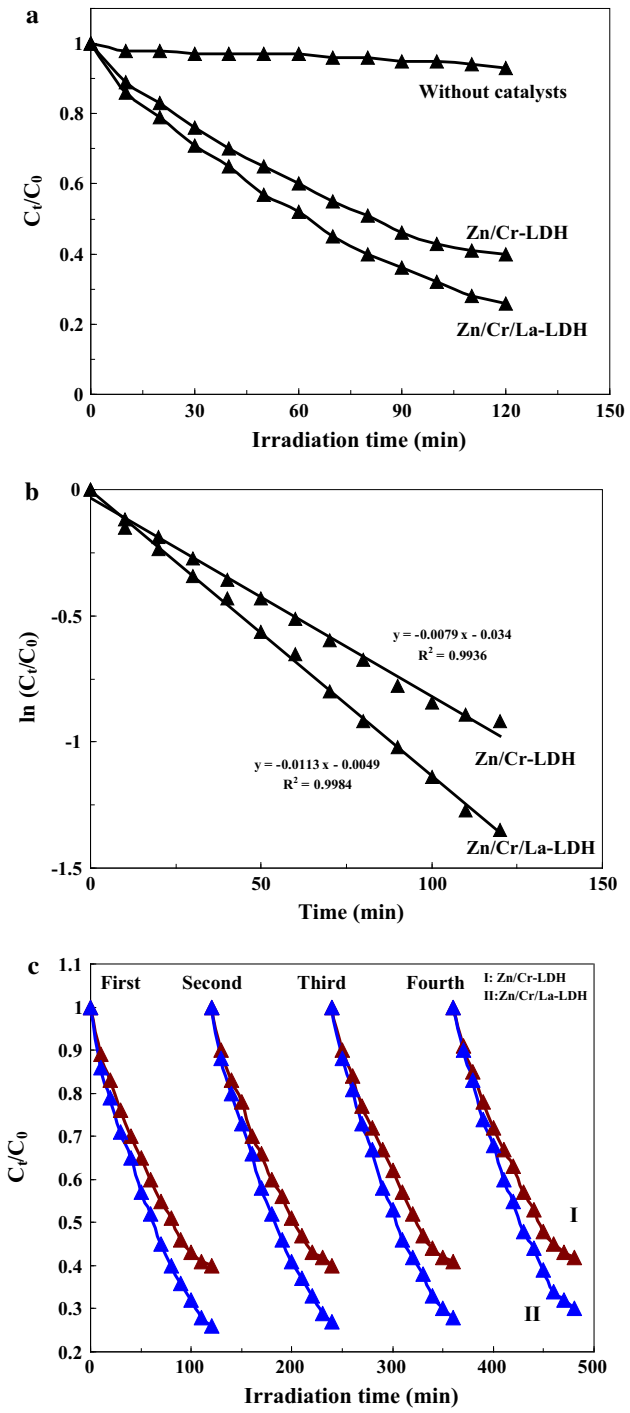

Fig. 7 **a** The photo catalytic degradation of MB over Zn/Cr-LDH and Zn/Cr/La-LDH samples under xenon light irradiation. **b** Ln(C_t/C_0) versus irradiation time plot. **c** Photo catalyst stability test of prepared samples

$$\text{Photo degradation yield}\,(\%) = [(C_0 - C)/C_0] \times 100 \quad (1)$$

where C_0 and C are initial concentration and concentration of dyes after photo degradation under visible light irradiation at various time interval, respectively. In order to obtain the real photo degradation yield, the decreases of the dye concentration because of the adsorption and direct photolysis should be deducted. The photo catalysis of MB is negligible without the presence of Zn/Cr-LDH and Zn/Cr/La-LDH samples, suggesting that the degradation of MB is induced by photo catalysis. Figure 7a shows the photo degradation rate of MB under Xe light in presence of different samples. Under the irradiation of light, the Zn/Cr/La-LDH sample exhibited better photo catalytic activity than Zn/Cr-LDH sample. The higher photo catalytic activity of Zn/Cr/La-LDH sample can be attributed to the combined effect of various factors: the presence of lanthanum, the effect of surface morphology on the surface area of these samples and the increased light-harvesting ability (capability to absorb visible light and higher light absorption, compared to Zn/Cr-LDH). Photo catalytic reactions kinetics can be expressed by the Langmuir–Hinshelwood (L–H) model [39, 40]:

$$\ln(C_0/C) = k_{app}t \quad (2)$$

where kapp is the apparent pseudo first order reaction rate constant and t is the reaction time. A plot of $\ln(C_0/C)$ versus t will yield a slope of k_{app}. The calculated kapp and correlation coefficients were present in the Fig. 7b. The degradation process follows pseudo first-order kinetics and the degradation rate constant calculated from the slope of the kinetics plot was found to be 0.0079 and 0.0113 min^{-1} for Zn/Cr-LDH and Zn/Cr/La-LDH samples, respectively. The stability of a photo catalyst is also important for its practical application for it can be regenerated and reused.

The stability and reusability of the Zn/Cr-LDH and Zn/Cr/La-LDH catalysts was carried out with the same ratio of catalyst and dye concentration. After each reaction run, the catalyst was separated from the reaction system and its reusability was also investigated carefully. The catalyst was washed several times with distilled water, dried and reused. Each cycle was carried out in the dark for 120 min and then exposed under Xe light for 120 min. As shown in Fig. 7c, after a four-cycle experiment, these catalysts exhibited similar catalytic performance without significant deactivation. The above results revealed that these composite are potential catalysts with good photo catalytic activity, stability, and reusability.

4 Conclusions

In summary, Zn/Cr-LDH and Zn/Cr/La-LDH composites were synthesized by co-precipitation method. The characteristics of the obtained samples were investigated by SEM, TEM, XRD, FTIR, EDX and UV–Vis. Photo catalytic experiments showed that lanthanum containing ZnCr-Layered double hydroxide (Zn/Cr/La-LDH) catalyst

displayed high photo catalytic activity as compared to Zn/Cr-LDH under xenon light irradiation because of the increased surface area and light harvesting ability. Kinetic research showed that the reaction rate constant of Zn/Cr/La-LDH sample is approximately 1.4 times higher than the reaction rate constant of Zn/Cr-LDH. The stability of the samples indicated no observable performance degradation for prepared photo catalyst even after four recycles. Therefore, these prepared composites would have a widely applied prospect in photo catalytic field to eliminate the organic pollutants from waste water.

Acknowledgments The authors are grateful to the Research Affairs Division Isfahan University of Technology (IUT), Isfahan, for partial financial support. Additional financial support from National Elite Foundation (NEF), and Iran Nanotechnology Initiative Council (INIC) is gratefully acknowledged.

Compliance with ethical standards

Conflict of interest The authors declare no competing financial interest.

References

1. N.T. Kim Phuong, M. Beak, B.T. Huy, Y. Lee, Adsorption and photodegradation kinetics of herbicide 2,4,5-trichlorophenoxyacetic acid with MgFeTi layered double hydroxides. Chemosphere **146**, 51–59 (2016)
2. J. Liua, G. Zhang, Recent advances in synthesis and applications of clay-based photocatalysts: a review. Phys. Chem. Chem. Phys. **16**, 8178–8192 (2014)
3. H.G. Kim, P.H. Borse, W. Choi, J.S. Lee, Photocatalytic Nanodiodes for Visible-Light Photocatalysis. Angew. Chem. Int. Ed. **44**, 4585–4589 (2005)
4. Y.H. Peng, G.F. Huang, W.Q. Huang, Visible-light absorption and photocatalytic activity of Cr-doped TiO_2 nanocrystal films. Adv. Powder Technol. **23**, 8–12 (2012)
5. F. Jiang, JYu. Jiao, Visible-light-driven photocatalytic properties of layered double hydroxide supported-Bi_2O_3 modified by Pd(II) for methylene blue. Adv. Powder Technol. **26**, 439–447 (2015)
6. N. Liang, J. Zai, M. Xu, Q. Zhu, X. Wei, X. Qian, Novel Bi_2S_3/$Bi_2O_2CO_3$ heterojunction photocatalysts with enhanced visible light responsive activity and wastewater treatment. J. Mater. Chem. A **2**, 4208–4216 (2014)
7. S. Sarina, R. Waclawik, H. EZhu, Photocatalysis on supported gold and silver nanoparticles under ultraviolet and visible light irradiation. Green Chem. **15**, 1814–1833 (2014)
8. X. Chen, J. Wei, R. Hou, X. Zhang, H. Wang, Growth of g-C_3N_4 on mesoporous TiO_2 spheres with high photocatalytic activity under visible light irradiation. Appl. Catal. B: Environ. **188**, 342–350 (2016)
9. M. Shanmugam, A. Alsalme, A. Alghamdi, R. Jayavel, Enhanced photocatalytic performance of the graphene-V_2O_5 nanocomposite in the degradation of methylene blue dye under direct sunlight. ACS Appl. Mater. Interfacs **7**, 14905–14911 (2015)
10. P.K. Boruah, P. Borthakur, G. Darabdhara, D. Saikia, M.R. Das, Sunlight assisted degradation of dye molecules and reduction of toxic Cr(VI) in aqueous medium using magnetically recoverable Fe3O4/reduced graphene oxide nanocomposite. RSC Adv. **6**, 11049–11063 (2016)
11. Y.F. Sun, S. Gao, Y. Xie, Atomically-thick two-dimensional crystals: electronic structure regulation and energy device construction. Chem. Soc. Rev. **43**, 530–546 (2014)
12. L. Zhang, Z. Xiong, G. Zhao, Chapter 13: Hierarchical nanoheterostructures: layered double hydroxide-based photocatalysts, in *Green Photo-Active Nanomaterials: Sustainable Energy and Environmental Remediation*, RSC Green Chemistry, pp. 309–338 (2015)
13. S.J. Xia, F.X. Liu, Z.M. Ni, J.L. Xue, P.P. Qian, Ti-based layered double hydroxides: efficient photocatalysts for azo dyes degradation under visible light. Appl. Catal. B: Environ. **144**, 570–579 (2014)
14. Y. Xu, H. Hou, Q. Liu, L. Dou, G. Qian, Removal behavior research of orthophosphate by CaFe-layered double hydroxides. Desalination Water Treat. **57**, 7918–7925 (2016)
15. Y. Wang, Z. Wang, X. Wu, X. Liu, M. Li, Synergistic effect between strongly coupled CoAl layered double hydroxides and graphene for the electrocatalytic reduction of oxygen. Electrochim. Acta **192**, 196–204 (2016)
16. A.A. Ensafi, M. Jafari-Asl, A. Nabiyan, B. Rezaei, M. Dinari, Hydrogen storage in hybrid of layered double hydroxides/reduced graphene oxide using spillover mechanism. Energy **99**, 103–114 (2016)
17. K. Zargoosh, S. Kondori, M. Dinari, S. Mallakpour, Synthesis of layered double hydroxides containing a biodegradable amino acid derivative and their application for effective removal of cyanide from industrial wastes. Ind. Eng. Chem. Res. **54**, 1093–1102 (2015)
18. C. Li, M. Wei, D.G. Evans, X. Duan, Layered double hydroxide-based nanomaterials as highly efficient catalysts and adsorbents. Small **10**, 4469–4486 (2014)
19. T. Selvam, A. Inayat, W. Schwieger, Reactivity and applications of layered silicates and layered double hydroxides. Dalton Trans. **43**, 10365–10387 (2014)
20. X. Ruan, S. Huang, H. Chen, G. Qian, Sorption of aqueous organic contaminants onto dodecyl sulfate intercalated magnesium iron layered double hydroxide. Appl. Clay Sci. **72**, 96–103 (2013)
21. H. Chen, G. Qian, X. Ruan, R.L. Frost, Abatement of aqueous anionic contaminants by thermo-responsive nanocomposites: (poly(N-isopropylacrylamide))-co-silylanized Magnesium/Aluminun layered double hydroxides. J. Colloid Interface Sci. **448**, 65–72 (2015)
22. M. Dinari, P. Asadi, S. Khajeh, In situ thermal synthesis of novel polyimide nanocomposite films containing organo-modified layered double hydroxide: morphological, thermal and mechanical properties. New J. Chem. **39**, 8195–8203 (2015)
23. J. Li, Q. Fan, Y. Wu, Z. Tang, X. Wang, Magnetic polydopamine decorated with Mg-Al LDH nanoflakes as a novel bio-based adsorbent for simultaneous removal of potentially toxic metals and anionic dyes. J. Mater. Chem. A. **4**, 1737–1746 (2016)
24. Q. Wang, D. Ohare, Recent advances in the synthesis and application of layered double hydroxide (LDH) nanosheets. Chem. Rev. **112**, 4124–4155 (2012)
25. S. Mallakpour, M. Dinari, Facile synthesis of nanocomposite materials by intercalating an optically active poly (amide-imide) enclosing (L)-isoleucine moieties and azobenzene side groups into a chiral layered double hydroxide. Polymer **54**, 2907–2916 (2013)
26. S. Mallakpour, M. Dinari, Novel bionanocomposites of poly (vinyl alcohol) and modified chiral layered double hydroxides: synthesis, properties and a morphological study. Prog. Org. Coat. **77**, 583–589 (2014)
27. S. Mallakpour, M. Dinari, Ultrasound-assisted one-pot preparation of organo-modified nano-sized layered double hydroxide and

its nanocomposites with polyvinylpyrrolidone. J. Polym. Res. **21**, 1–8 (2014)
28. G. Nagaraju, G.S.R. Raju, Y.H. Ko, J.S. Yu, Hierarchical Ni-Co layered double hydroxide nanosheets entrapped on conductive textile fibers: a cost-effective and flexible electrode for high-performance pseudocapacitors. Nanoscale **8**, 812–825 (2016)
29. J. Qu, Q. Zhang, X. Li, X. He, S. Song, Mechanochemical approaches to synthesize layered double hydroxides: a review. Appl. Clay Sci. **119**, 185–192 (2016)
30. Y. Zhao, X. Jia, G.I.N. Waterhouse, L.Z. Wu, C.H. Tung, D. O'Hare, Tierui Zhang, Layered double hydroxide nanostructured photocatalysts for renewable energy production. Adv. Energy Mater. **1501974**, 1–20 (2015)
31. P.R. Chowdhurya, K.G. Bhattacharyya, Ni/Ti layered double hydroxide: synthesis, characterization and application as a photocatalyst for visible light degradation of aqueous methylene blue. Dalton Trans. **44**, 6809–6824 (2015)
32. J. Yu, L. Lu, J. Li, P. Song, Biotemplated hierarchical porous-structure of ZnAl-LDH/$ZnCo_2O_4$ composites with enhanced adsorption and photocatalytic performance. RSC Adv. **6**, 12797–12808 (2016)
33. Y. Guo, Z. Zhu, Y. Qiu, J. Zhao, Adsorption of arsenate on Cu/Mg/Fe/La layered double hydroxide from aqueous solutions. J. Hazard. Mater. **239–240**, 279–288 (2012)
34. H. Jun, Z. Zhiliang, L. Hongtao, Q. Yanling, Effect of metal composition in lanthanum-doped ferric-based layered double hydroxides and their calcined products on adsorption of arsenate. RSC Adv. **4**, 5156–5164 (2014)
35. S. Li, H. Qin, R. Zuo, Z. Bai, Friction properties of La-doped Mg/Al layered double hydroxide and intercalated product as lubricant additives. Tribology Int. **191**, 60–66 (2015)
36. C. Busetto, G.P. Del, G. Mamara, F. Trifiro, A. Vaccari, Catalysts for lowtemperature methanol synthesis, Preparation of Cu–Zn–Al mixed oxides via hydrotalcite-like precursors. J. Catal. **85**, 260–266 (1984)
37. I. Cota, E. Ramírez, F. Medina, G. Layrac, D. Tichit, C. Gérardin, Influence of the preparation route on the basicity of La-containing mixed oxides obtained from LDH precursors. J. Molecular Catal. A. Chem. **412**, 101–106 (2016)
38. S. Mallakpour, M. Dinari, Enhancement in thermal properties of poly(vinyl alcohol) nanocomposites reinforced with Al_2O_3 nanoparticles. J. Reinf. Plast. Comps. **32**, 217–224 (2013)
39. M.M. Momeni, Y. Ghayeb, Photochemical deposition of platinum on titanium dioxide-tungsten trioxide nanocomposites: an efficient photocatalyst under visible light irradiation. J. Mater. Sci.: Mater. Electron. **27**, 1062–1069 (2016)
40. M.M. Momeni, Y. Ghayeb, Fabrication and characterization of zinc oxide-decorated titania nanoporous by electrochemical anodizing-chemical bath deposition techniques: visible light active photocatalysts with good stability. J. Iran. Chem. Soc. **13**, 481–488 (2016)